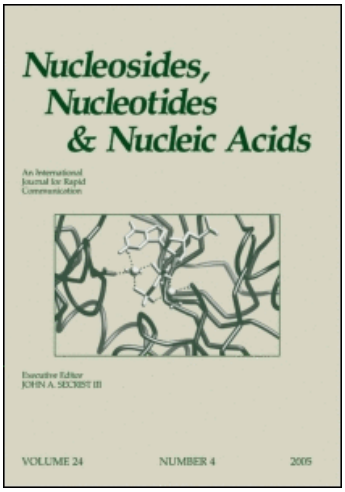

Nucleosides, Nucleotides and Nucleic Acids
Publication details, including instructions for authors and subscription information:
http://www.informaworld.com/smpp/title~content=t713597286

E. coli RNase HI and the Phosphonate-DNA/RNA Hybrid: Molecular Dynamics Simulations

I. Barvík Jr.[a]
[a] Facultu of Mathematics and Physics, Institute of Physics, Charles University, Prague 2, Czech Republic

To cite this Article Barvík Jr., I.(2005) '*E. coli* RNase HI and the Phosphonate-DNA/RNA Hybrid: Molecular Dynamics Simulations', Nucleosides, Nucleotides and Nucleic Acids, 24: 5, 435 — 441
To link to this Article: DOI: 10.1081/NCN-200059984
URL: http://dx.doi.org/10.1081/NCN-200059984

Nucleosides, Nucleotides, and Nucleic Acids, 24 (5–7):435–441, (2005)

ISSN: 1525-7770 print/ 1532-2335 online
DOI: 10.1081/NCN-200059984

Taylor & Francis
Taylor & Francis Group

E. COLI RNASE HI AND THE PHOSPHONATE-DNA/RNA HYBRID: MOLECULAR DYNAMICS SIMULATIONS

I. Barvík Jr. ▫ *Faculty of Mathematics and Physics, Institute of Physics, Charles University, Prague 2, Czech Republic*

▫ *A model for the complex between E. coli RNase HI and the DNA/RNA hybrid (previously refined by molecular dynamics simulations) was used to determine the impact of the internucleotide linkage modifications (either 3′–O–CH_2–P–O–5′ or 3′–O–P–CH_2–O–5′) on the ability of the modified-DNA/RNA hybrid to create a complex with the protein. Modified internucleotide linkages were incorporated systematically at different positions close to the 3′-end of the DNA strand to interfere with the DNA binding site of RNase H. Altogether, six trajectories were produced (length 1.5ns). Mutual hydrogen bonds connecting both strands of the nucleic acids hybrid, DNA with RNase H, RNA with RNase H, and the scissile bond with the $Mg^{++}\cdot 4H_2O$ chelate complex (bound in the active site) were analyzed in detail. Many residues were involved in binding of the DNA (Arg88, Asn84, Trp85, Trp104, Tyr73, Lys99, Asn100, Thr43, and Asn16) and RNA (Gln76, Gln72, Tyr73, Lys122, Glu48, Asn44, and Cys13) strand to the substrate-binding site of the RNase H enzyme. The most remarkable disturbance of the hydrogen bonding net was observed for structures with modified internucleotide linkages positioned in a way to interact with the Trp104, Tyr73, Lys99, and Asn100 residues (situated in the middle of the DNA binding site, where a cluster of Trp residues forms a rigid core of the protein structure).*

Keywords Molecular Dynamics, Antisense, RNase H

INTRODUCTION

An effective in vivo use of oligonucleotides as antisense compounds requires their stability towards nucleases in biological fluids, sufficient affinity to the target sequences, and elicitation of RNase H activity. A number of phosphonate-based mononucleotide analogs containing an O-(phosphono)methyl groups instead of the natural phosphonomonoester one were found to be potent antivirals.[1] This indicated enzyme stability of the phosphonate –O–P–CH_2–O– bond. Several structural variants of dT_{15} and dA_{15} analogs containing isopolar, nonisosteric,

This work was supported by the Grant Agency of Czech Republic (project No. 202/02/D114).
Received October 2004, accepted January 2005.
Address correspondence to I. Barvík, Jr., Institute of Physics, Charles University, Ke Karlovu 5, 121 16 Prague 2, Czech Republic; Fax: +420-224-922-797; E-mail: ibarvik@karlov.mff.cuni.cz

phosphonate, internucleotide linkages (either the 3′–O–P–CH_2–O–5′ or 3′–O–CH_2–P–O–5′ type) were synthesized.[2] Apart from confirming superior nucleolytic stabilities of these oligonucleotide analogs in L1210 cell free extract and in nuclease assays, it was found that all-phosphonate oligomers mostly form weaker complexes with natural counterparts than phosphorothioate ones, but in the mode of alternating phosphonate-phosphodiester internucleotide linkages mostly surpass the phosphorothioate oligodeoxynucleotides. In addition, a protective effect of phosphonate linkages on the neighbor phosphodiester ones against nuclease cleavage was found. Oligonucleotides consisting of both the 3′–O–P–CH_2–O–5′ and phosphodiester linkages are capable to elicit RNase H activity (in contrast to the 3′–O–CH_2–P–O–5′). The oligodeoxyadenosine with either 3′–O–P–CH_2–O–5′ or 3′–O–CH_2–P–O–5′ linkage has been investigated by using molecular dynamics (MD) simulations.[3–6] Further, a model for the complex between *E. coli* RNase HI and the DNA/RNA hybrid was refined by molecular dynamics simulations with explicit inclusion of solvent molecules.[7] The $rA_5 \cdot dT_5$ hybrid found (within a 9-ns MD run) suitable cavity formed by Trp residues and so called basic protrusion, where the DNA backbone was tightly accommodated. Thereafter, elongated $rA_{15} \cdot dT_{15}$ duplex structure was able to bind simultaneously into the mentioned cavity (DNA strand) and the active place of RNase HI (RNA strand). The 5-ns MD simulation has demonstrated outright stability (and reliability) of the proposed model. Now we proceed toward a investigation of the RNase H + modified-DNA:RNA complex using phosphonate nucleic acids and well characterized *E. coli* RNase HI.[8,9] Conclusions gained for *E. coli* RNase HI are supposed to be transmittable (in some measure) to human RNase H. The carboxyl terminus of human RNaseHI is highly conserved with *E. coli* RNase HI and contains the amino acid residues of the putative catalytic site and basic substrate-binding domain of the *E. coli* RNase H enzyme.[10]

METHODOLOGY

Initial structures were derived from the recently determined $rA_{15} \cdot T_{15}$+ RNase H model.[7] Five base pairs not participating in the DNA:RNA hybrid binding toward the enzyme were omitted from the simulated system. Modified internucleotide linkages (either 3–O–CH_2–P–O–5 or 3–O–P–CH_2–O–5) were incorporated by hand into the DNA strand: 1) 5′-TTTTTTTT-PC-TT-3′ (3CP5_A), 2) 5′-TTTTTTT-PC-TTT-3′ (3CP5_B), 3) 5′-TTTTTT-PC-TTTT-3′ (3CP5_C), 4) 5′-TTTTTTTT-CP-TT-3′ (3PC5_A), 5) 5′-TTTTTTT-CP-TTT-3′ (3PC5_B), 6) 5′-TTTTTT-CP-TTTT-3′ (3PC5_C). Produced coordinate. PDB files were used as input files for AMBER 5.0 software package. The complex was surrounded by TIP3P water molecules. This leads to a periodic box size of ~70 Å by ~50 Å by ~40 Å. Fully solvated trajectories were computed by using the SANDER module of the AMBER 5.0 software package. Usual computational procedures and equilibration protocol were used.[11] Dynamical motion of the structure within MD

runs was visualized by using the VMD software package. Time development of the torsion angle parameters, Watson-Crick hydrogen bonding, sugar conformations, etc., were resolved by means of the CARNAL module.

RESULTS

Watson-Crick Hydrogen Bond Connection

Mean values of hydrogen bonds obtained for individual base-pairs by averaging over the whole MD trajectory are shown in Table 1. In the free $dA_x \cdot dT_x$ duplexes the average hydrogen bond lengths are usually uniformly 1.9–2.0 Å as the the relevant proton-acceptor distances fluctuate in the interval ranging from 1.7 to 2.5 Å. Heightened values determined for terminal base pairs (for example A10–T1 in 3CP5_A) are rather common observations as the ends of double helical structures are transiently frayed from time to time. On the other hand, in the case of central base pairs heightened lengths indicate adaptation of the nucleic acids structure to the shape of the substrate binding site of the enzyme. There are two such segments, A2–T9, A3–T8 base pairs, carrying chemical modifications in the DNA strand, and A6–T5, A7–T4 base pairs, where the A6 and A7 residues are involved in the binding toward the enzyme. The most remarkable disturbance of the hydrogen bond net was determined in the case of the A5–T6 base pair in 3CP5_C, where a transient interruption lasting for ~100 ps was observed. It was followed by remarkable failure in the DNA-protein as well as RNA-protein hydrogen bonding (described below). Remaining Watson-Crick hydrogen bonds in the DNA:RNA hybrids remained almost intact within the 1.5-ns MDs run at 300 K.

DNA Binding Site

In addition to steric and electrostatic complementarities between the molecular surfaces of the enzyme and the minor groove of the hybrid in the model, many

TABLE 1 Average Lengths (in Å) and Standard Deviations (Shown in Parentheses) of the Watson-Crick Hydrogen Bonds for Individual Base Pairs (Numbered from the 5′-End of the Adenosine Strand)

Distance (Å)	3CP5_A	3CP5_B	3CP5_C	3PC5_A	3PC5_B	3PC5_C
A1–T10	2.1 (0.3)	2.1 (0.2)	2.1 (0.3)	2.1 (0.4)	2.0 (0.2)	2.1 (0.2)
A2–T9	2.0 (0.2)	2.0 (0.1)	2.1 (0.2)	2.1 (0.2)	2.0 (0.1)	2.0 (0.2)
A3–T8	2.0 (0.1)	2.1 (0.2)	2.0 (0.2)	2.0 (0.1)	2.0 (0.2)	2.0 (0.1)
A4–T7	2.0 (0.1)	2.0 (0.1)	2.0 (0.1)	2.0 (0.1)	2.0 (0.1)	2.0 (0.1)
A5–T6	1.9 (0.1)	1.9 (0.1)	2.2 (0.9)	2.0 (0.1)	2.0 (0.1)	2.0 (0.1)
A6–T5	2.1 (0.3)	2.1 (0.3)	2.3 (0.3)	2.1 (0.2)	2.2 (0.3)	2.0 (0.1)
A7–T4	2.2 (0.4)	2.2 (0.3)	2.2 (0.2)	2.2 (0.2)	2.2 (0.2)	2.2 (0.3)
A8–T3	2.0 (0.1)	2.0 (0.1)	2.0 (0.1)	2.0 (0.1)	2.0 (0.1)	2.0 (0.1)
A9–T2	1.9 (0.1)	2.0 (0.1)	2.0 (0.1)	2.0 (0.1)	2.0 (0.1)	2.0 (0.1)
A10–T1	4.6 (1.0)	2.0 (0.1)	2.0 (0.1)	2.0 (0.2)	2.0 (0.3)	2.0 (0.2)

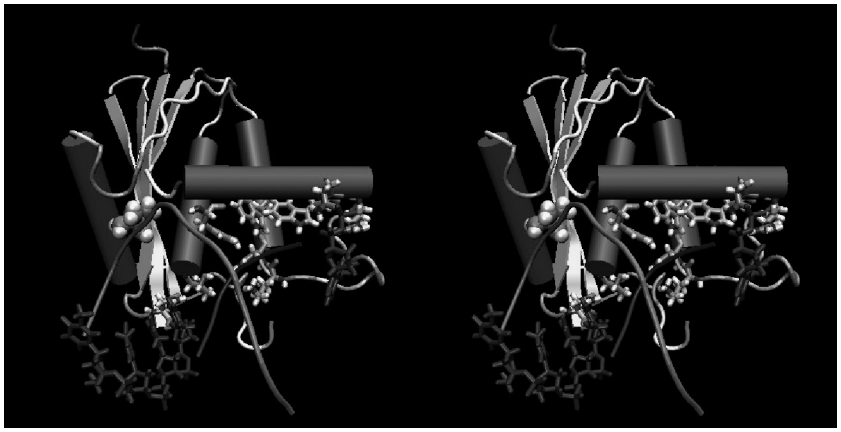

FIGURE 1 A model for the complex between *E. coli* RNase HI and $rA_{10}\cdot dT_{10}$. DNA binding site residues are highlighted. RNA and the part of DNA interacting with the DNA binding site are shown as ribbons for clarity.

residues were found to be involved in hydrogen bonding of the DNA strand to the RNase H enzyme within MD runs (Figure 1, Table 2). In particular Arg88, Asn84, Trp85, Trp104, Tyr73, Lys99, Asn100, Thr43, Asn16, and T5–T9 phosphate groups should be mentioned. In fact, Arg88 and Asn84 give steady stabilization only to 3CP5_B and 3PC5_C structures. On the other hand, Thr43 and Asn16 were found as potent stabilizers; however, they interfere with natural T6–T5 and T5–T4 internucleotide linkages. Remaining anchors (Trp85, Trp104, Tyr73, Lys99, and Asn100) were disturbed by transient breakage of the A5–T6 base pair in 3CP5_C. It should be mentioned that Lys99 and Asn100 bind phosphate groups in both T7–T6 and T6–T5 internucleotide linkages. Summarized, DNA strands (with the exception of 3CP5_C) were tightly anchored to the DNA binding site of the protein adjacent to the Trp cluster (Trp81, Trp85, Trp90, and Trp104) forming the rigid core of the RNase H structure.

RNA Binding Site

Similarly, many hydrogen bonds between the Gln76, Gln72, Tyr73, Lys122, Glu48, Asn44, and Cys13 residues and the A5–A8 segment of the RNA strand

TABLE 2 Average Distances (in Å) and Standard Deviations (Shown in Parentheses) Between Groups of Atoms Connecting by Hydrogen Bonds DNA and the RNase H Substrate Binding Site

Distance (Å)	3CP5_A	3CP5_B	3CP5_C	3PC5_A	3PC5_B	3PC5_C
A5 N3-NE2 Gln76	3.1 (0.2)	3.1 (0.2)	4.1 (1.2)	3.1 (0.3)	3.1 (0.2)	3.2 (0.3)
A6 P-NE2 Gln72	3.6 (0.2)	4.6 (0.7)	4.2 (0.5)	4.0 (0.6)	4.0 (0.6)	3.9 (0.6)
A6 C2-N Tyr73	4.1 (0.2)	4.0 (0.2)	4.1 (0.2)	4.1 (0.2)	4.0 (0.2)	4.1 (0.3)
A6 P-NZ Lys122	5.9 (1.6)	3.9 (0.4)	3.9 (0.5)	4.8 (1.3)	4.8 (1.3)	6.7 (3.0)
A7 O2′-CD Glu48	3.3 (0.3)	3.4 (0.3)	3.6 (0.4)	3.3 (0.2)	3.4 (0.2)	3.4 (0.3)
A7 O2′-ND2 Asn44	2.9 (0.1)	3.0 (0.2)	2.9 (0.1)	2.9 (0.1)	2.9 (0.1)	3.0 (0.2)
A8 O2′-O Cys13	3.0 (0.2)	2.9 (0.2)	2.9 (0.2)	2.9 (0.2)	2.9 (0.2)	3.1 (0.5)

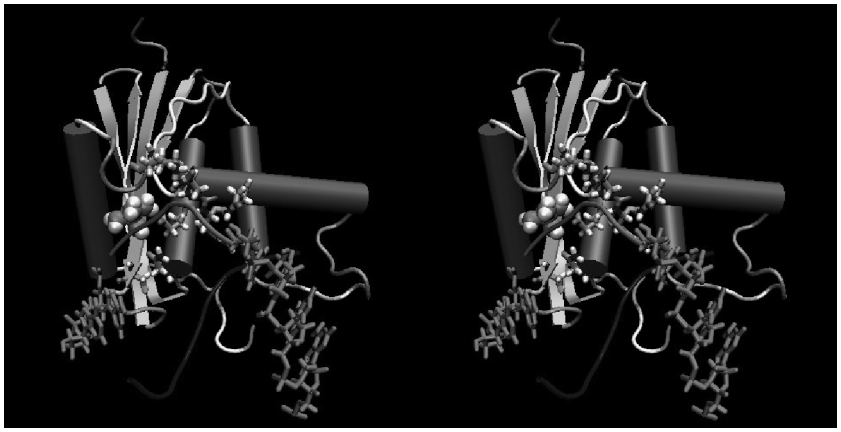

FIGURE 2 A model for the complex between *E. coli* RNase HI and $rA_{10}\cdot dT_{10}$. RNA binding site residues are highlighted. DNA and the part of RNA interacting with the RNA binding site are shown as ribbons for clarity.

were established within MD runs (Figure 2, Table 3). It should be noted, that riboses of the A7–A8 internucleotide linkage situated in the active site (scissile by the enzyme) are included in the hydrogen bond net. Gln 72 (good for 3CP5_A) and Lys122 (functional in 3CP5_B and 3CP5_C) were found as rather poor binders. On the other hand, Asn44 unhesitatingly anchors all examined structures. Marks of the A5–T6 hydrogen bonding instability can be found in 3CP5_C.

$Mg^{2+} + 4 \cdot H_2O$ and O3′-A7 Contact

Asp 10, Gly11, and Asp70 residues were used to anchor the Mg^{2+} ion (essential for a proper enzyme action) into the active site within MD simulations. Further, four water molecules were added to fill up coordination sites of the ion. They served as mediators of interaction with the Glu48 and Asp134 residues bringing auxiliary

TABLE 3 Average Distances (in Å) and Standard Deviations (Shown in Parentheses) Between Groups of Atoms Connecting by Hydrogen Bonds RNA and the RNase H Substrate Binding Site

Distance (Å)	3CP5_A	3CP5_B	3CP5_C	3PC5_A	3PC5_B	3PC5_C
T9 P–NH1 Arg88	3.9 (0.4)	4.0 (0.2)	4.5 (1.4)	6.1 (1.9)	5.9 (1.2)	4.0 (0.4)
T9 P–NH2 Arg88	4.2 (0.5)	4.0 (0.2)	4.5 (1.5)	6.7 (2.7)	6.3 (1.0)	3.9 (0.3)
T9 P–ND2 Asn84	4.9 (0.7)	3.9 (0.6)	4.4 (0.9)	4.9 (1.0)	5.0 (1.0)	3.9 (0.7)
T8 P–NE1 Trp85	3.9 (0.1)	4.1 (0.1)	3.9 (0.3)	4.0 (0.2)	3.9 (0.2)	3.9 (0.1)
T7 P–NE1 Trp104	4.3 (0.2)	4.3 (0.1)	4.1 (0.3)	4.3 (0.1)	4.3 (0.1)	4.3 (0.1)
T7 P–OH Tyr73	3.8 (0.2)	3.8 (0.2)	4.6 (0.4)	3.8 (0.2)	3.8 (0.2)	3.9 (0.5)
T7 P–NZ Lys99	4.1 (0.1)	4.1 (0.1)	4.3 (0.7)	4.1 (0.1)	4.1 (0.1)	4.0 (0.1)
T7 P–ND2 Asn100	3.7 (0.2)	3.7 (0.2)	3.8 (0.2)	3.7 (0.2)	3.6 (0.2)	3.8 (0.1)
T6 P–NZ Lys99	3.6 (0.1)	3.6 (0.1)	3.7 (0.3)	3.6 (0.2)	3.6 (0.1)	3.5 (0.2)
T6 P–ND2 Asn100	3.7 (0.2)	3.8 (0.2)	3.9 (0.3)	3.8 (0.3)	3.7 (0.2)	3.7 (0.2)
T6 P–OG1 Thr43	3.8 (0.2)	3.7 (0.1)	3.8 (0.2)	3.8 (0.2)	3.7 (0.1)	3.8 (0.2)
T5 O4′–ND2 Asn16	3.0 (0.2)	2.9 (0.1)	3.0 (0.2)	2.9 (0.1)	3.0 (0.2)	3.0 (0.2)

TABLE 4 Average Distances (in Å) and Standard Deviations (Shown in Parentheses) Between Mg^{2+}+4 · H_2O Chelate and O3′-A7 Oxygen

Distance (Å)	3CP5_A	3CP5_B	3CP5_C	3PC5_A	3PC5_B	3PC5_C
Mg, O3′ A7	3.8 (0.2)	3.7 (0.1)	3.8 (0.2)	3.7 (0.2)	3.8 (0.2)	4.1 (0.4)
W1 O, O3′ A7	4.3 (0.4)	4.4 (0.3)	4.4 (0.3)	4.4 (0.2)	4.4 (0.2)	4.3 (0.4)
W2 O, O3′ A7	4.0 (0.4)	3.8 (0.2)	3.9 (0.3)	3.8 (0.2)	3.9 (0.2)	4.5 (0.7)
W3 O, O3′ A7	3.1 (0.2)	3.1 (0.2)	3.3 (0.2)	3.1 (0.2)	3.2 (0.3)	3.6 (0.7)
W4 O, O3′ A7	3.0 (0.2)	2.8 (0.1)	2.8 (0.2)	2.9 (0.2)	2.9 (0.2)	3.0 (0.3)

stabilization into the complex. Distances between the O3′ oxygen from the A7–A8 scissile internucleotide linkage on the one hand and Mg^{2+} and water molecules (forming chelate complex bound in the active site) represented by oxygens on the other hand were analyzed in detail to uncover potential displacements in consequence of chemical modifications of the DNA strand (Table 4). Surprisingly, it was found only in the case of the 3PC5_C structure, which seemed to be non-problematic up to now.

CONCLUSIONS

Both structures (3CP5_C and 3PC5_C) carrying modified internucleotide linkages positioned in the nearby of Trp104, Tyr73, Lys99, and Asn100 residues, where a cluster of Trp residues forms a rigid core of the protein structure, exhibited poorer ability to bind to RNase H. In the case of the 3CP5_C structure Watson-Crick, DNA-protein as well as RNA-protein hydrogen bonding was disturbed. In the case of the 3PC5_C structure rather positioning of the RNA strand into the active site was changed within a MD simulation. Therefore, steric compatibilities in the middle of the DNA binding site seem to be the most crucial for proper positioning of the antisense DNA strand enabling efficient enzymatic cleavage of the RNA strand.

REFERENCES

1. De Clercq, E.; Holý, A.; Rosenberg, I. Efficacy of phosphonylmethoxyalkyl derivatives of adenine in experimental herpes-simplex virus and vaccinia virus-infections in vivo. Antimicrob. Agents Chemother. **1989**, *33*, 185–191.
2. Rejman, D.; Snášel, J.; Liboska, R.; Točík, Z.; Pačes, O.; Králíková, S.; Rinnová, M.; Kois, P.; Rosenberg, I. Oligonucleotides with isopolar phosphonate internucleotide linkage: a new perspective for antisense compounds? Nucleosides Nucleotides Nucleic Acids **2001**, *20*(4–7), 819–823.
3. Barvík, I., Jr.; Štěpánek, J.; Bok, J. Explicit solvent molecular dynamics simulation of a duplex formed by a modified oligonucleotide with alternating phosphate/phosphonate internucleoside linkages and its natural counterpart. J. Biomol. Struct. Dyn. **2002**, *19*, 863–875.
4. Barvík, I., Jr.; Štěpánek, J.; Bok, J. Fully solvated molecular dynamics simulations of duplexes formed by modified oligonucleotides with xylo/phosphodiesteric and xylo/phosphonate internucleotide linkages and its natural counterpart. Comput. Phys. Commun. **2002**, *147*, 158–161.
5. Hanuš, J.; Barvík, I., Jr.; Štepánek, J.; Turpin, P.Y.; Bok, J.; Rosenberg, I.; Petrová, M. The CH2-lengthening of the internucleotide linkage in ApA dimer can improve its conformational compatibility with its natural polynucleotide counterpart. Nucleic Acids Res. **2001**, *29*, 5182–5194.

6. Barvík, I., Jr.; Štěpánek, J.; Bok, J. Molecular dynamics simulations of the oligonucleotide with the modified phosphate/phosphonate internucleotide linkage. Czechoslov. J. Phys. **1998**, *48*, 409–415.
7. Barvík, I., Jr. Model for the complex between *E. coli* RNase HI and the DNA/RNA hybrid refined by molecular dynamics simulations. J. Biomol. Struct. Dyn. Submitted
8. Nakamura, H.; Oda, Y.; Iwai, S.; Inoue, H.; Ohtsuka, E.; Kanaya, S.; Kimura, S.; Katsuda, C.; Katayanagi, K.; Morikawa, K.; Miyashiro, H.; Ikehara, M. How does RNase H recognize a DNA · RNA hybrid. Proc. Natl. Acad. Sci. **1991**, *88*, 11535–11539.
9. Katayanagi, K.; Miyagawa, M.; Matsushima, M.; Ishikawa, M.; Kanaya, S.; Nakamura, H.; Ikehara, M.; Matsuzaki, T.; Morikawa, K. Structural details of ribonuclease H form *Escherichia coli* as refined to an atomic resolution. J. Mol. Biol. **1992**, *223*, 1029–1052.
10. Wu, H.; Lima, W.F.; Crooke, S.T. Investigating the structure of human RNase H1 by site-directed mutagenesis. J. Biol. Chem. **2001**, *276*, 23547–23553.
11. http://www.amber.ucsf.edu/amber/tutorial/polyA-polyT.